On the Performance of HARQ in IoT Networking with UAV-mounted Reconfigurable Intelligent Surfaces

Dimitrios Tyrovolas*, Prodromos-Vasileios Mekikis*, Sotiris A. Tegos*,
Panagiotis D. Diamantoulakis*, Christos K. Liaskos†, George K. Karagiannidis*
*Department of Electrical and Computer Engineering, Aristotle University of Thessaloniki (AUTh), Thessaloniki, Greece
e-mail: {tyrovolas, vmekikis, tegosoti, padiaman, geokarag}@auth.gr
†Computer Science Engineering Department, University of Ioannina, Ioannina, Greece.
e-mail: cliaskos@cse.uoi.gr

2022 IEEE 95th Vehicular Technology Conference (VTC2022-Spring) | 978-1-6654-8243-1/22/$31.00 ©2022 IEEE | DOI: 10.1109/VTC2022-Spring54318.2022.9860606

***Abstract*—Massive IoT deployments in smart cities pose a significant challenge to the data collection due to the harsh wireless channel conditions of dense urban environments. Aerial reconfigurable intelligent surfaces (RIS) carried by Unmanned Aerial Vehicles (UAVs) can improve the communication thanks to their high mobility that provides line-of-sight propagation. In this paper, we investigate the impact of the aerial RIS in the data collection by deriving the outage probability of the randomly-deployed devices, while taking into account the imperfect channel state and the UAV fluctuations. Furthermore, we study the effects on the network reliability of two hybrid automatic repeat request protocol types, i.e., incremental redundancy and code combining, as well as on the average throughput. Finally, we provide useful insights regarding the RIS characteristics that guarantee the optimal network performance.**

***Index Terms*—Reconfigurable Intelligent Surfaces (RIS), Unmanned Aerial Vehicles (UAVs), Coverage probability, Hybrid automatic repeat request (HARQ), Random deployment**

I. Introduction

During the last few years, massive Internet of Things (IoT) deployments have emerged as a means to efficiently communicate small amounts of data from vast numbers of low-cost wireless devices [1]. Megacities could be monitored using massive IoT by incorporating thousands or even millions of such devices and, then, process the generated big-data in specialized data-centers. However, due to heavy fading in dense urban environments and the fact that the numerous randomly-deployed wireless battery-powered IoT devices should be ultra-low power to guarantee low maintainability, novel flexible methods of data collection are inescapable.

At the same time, unmanned aerial vehicles (UAVs) are envisioned to play a pivotal role in future networks by providing high-speed and on-demand wireless connectivity [2]. Considering their flexible deployment, UAVs can assist in the data collection from randomly-deployed sensors due to the favorable characteristics of the established communication links in UAV-assisted networks. However, the effective utilization of UAVs depends on their flight time duration, which is limited by their battery capacity [3], [4]. Thus, it becomes of paramount importance to enhance the communication quality-of-service (QoS) in an energy-efficient way. To this end, UAVs can be used in combination with reconfigurable intelligent surfaces (RISs), which can facilitate the signal beamforming through their reflecting elements that can shift the phase of the reflected signals, without increasing the complexity at the UAV's side. Specifically, a synergetic UAV-RIS system could expand the wireless network's coverage in an energy-efficient way due to the nearly-passive nature of the RIS, which can modify its properties in an energy efficient manner [5], [6]. Furthermore, in order to exploit the UAVs' mobility, several works have examined synergetic UAV-RIS systems and shown their appealing characteristics in terms of rate and coverage probability [3], [7], [8].

Considering the city monitoring system could be delay-tolerant in certain use cases, the coverage can be even further improved by leveraging an error control protocol. Hence, the hybrid automatic repeat request (HARQ) protocol is able to achieve reliable data transmission by exploiting time diversity [9]. The advantage of HARQ is attributed to the retransmissions of the received packets that fail to be decoded with forward error correction (FEC). The combination of HARQ and RIS-assisted communication systems has been examined in [10], where it was shown that the utilization of HARQ can enhance the outage probability in a multi-RIS system. However, to the best of the authors' knowledge, the utilization of HARQ in a synergetic UAV-RIS system has not yet been examined.

Therefore, in this work, we study the communication performance of a system consisting of randomly-deployed IoT sensors and assisted by a UAV-mounted RIS. More specifically, our contribution is threefold: i) we derive a closed-form expression for the outage probability of a randomly-deployed IoT device, ii) we utilize the HARQ protocol and specifically HARQ with incremental redundancy (HARQ^{IR}) and HARQ with code combining (HARQ^{CC}) to enhance the performance and extract expressions for the outage probability and the average throughput, and iii) we provide a performance evaluation of the network.

The remaining part of this paper is organized as follows. The system model is described in Section II. The performance analysis of the considered network is presented in Section III-B and the numerical results in Section IV. Finally, Section V concludes the paper.

978-1-6654-8243-1/22/$31.00 ©2022 IEEE

II. System Model

We consider a set of uniformly-distributed IoT sensors located inside a disk of radius R. Due to the low-maintenance requirements of such sensors and in order to expand their lifetime, they are transmitting with ultra low-power. Therefore, we assume that there is no direct link to serve the communication between each sensor and the AP. To improve the received power at the AP, we employ a UAV-mounted RIS that is able to assist the communication by reflecting the sensor's transmissions towards the AP through a line-of-sight (LoS) link. Moreover, we assume that the UAV hovers at a height h from the disk's center and the mounted RIS consists of N reflecting elements. Considering the RIS reflection path, the baseband equivalent of the received symbol at the AP can be expressed as

$$Y = \sqrt{lGP_t}\sum_{i=1}^{N}|H_{i1}||H_{i2}|e^{-j(\omega_i+\arg(H_{i1})+\arg(H_{i2}))}X + W, \tag{1}$$

where X is the transmitted signal for which it is assumed that $\mathbb{E}[|X|^2] = 1$ with $\mathbb{E}[\cdot]$ and $\arg(\cdot)$ denoting expectation and the argument of a complex number, respectively. Also, P_t denotes the sensor transmit power, $G = G_tG_r$ is the product of the sensor and the AP antenna gains, and H_{i1} and H_{i2} are the complex channel coefficients that correspond to the i-th sensor-RIS and RIS-AP links, respectively. Moreover, W is the additive white Gaussian noise, ω_i is the phase correction term induced by the i-th reflecting element, and l is the path loss that correspond to the sensor-RIS and RIS-AP links, respectively. Specifically, l can be modeled as $l = C_0\left(\frac{d_0}{d_1d_2}\right)^n$, where n expresses the path loss exponent, C_0 denotes the product of the path loss of sensor-UAV and UAV-AP links at the reference distance d_0, while d_1 and d_2 denote the distances of the sensor-UAV and the UAV-AP links, respectively [11]. By taking into account the favorable characteristics of UAV communication links in cases where the UAV hovers in large heights, the path-loss exponent can be assumed to be equal to 2. Furthermore, it is assumed that there is no fading in the UAV-AP link regarding the characteristics of air-to-air channels as it is assumed that the AP is located at the top of a building (e.g. UAV charging station), thus $|H_{i2}| = 1$ and $\arg(H_{i2}) = \frac{2\pi r_i}{\lambda}$ with λ being the carrier's frequency wavelength and r_i the distance between the UAV and the i-th reflecting element. Considering that the AP is at the RIS's far-field, the distance r_i is approximately equal to d_2. Additionally, it is assumed that $|H_{i1}|$ is a random variable (RV) following the Nakagami-m distribution with shape parameter m and spread parameter Ω, which can describe accurately realistic communication scenarios characterized by severe or light fading. Finally, due to UAV fluctuations and imperfect CSI, each reflecting element does not adjust the phase perfectly to cancel the overall phase shift. Thus, the received signal at the AP can be rewritten as

$$Y = \sqrt{lGP_t}HX + W, \tag{2}$$

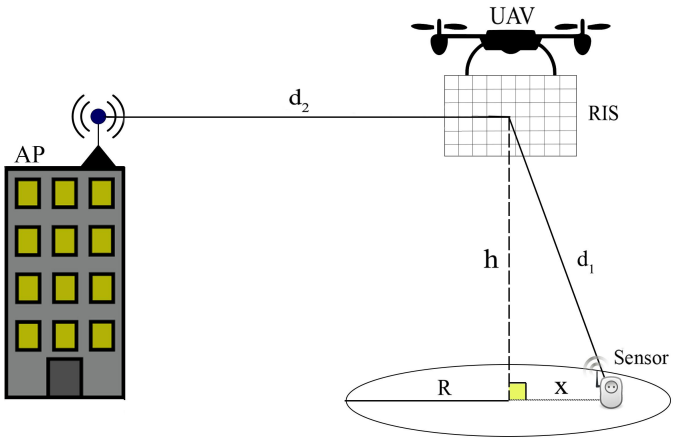

Fig. 1. Network topology.

where $H = \sum_{i=1}^{N}|H_{i1}|e^{-j\phi}$ and ϕ is an RV following the Von Mises distribution with concentration parameter κ. By taking into account the results found in [12], $\frac{1}{N}|H|$ can be approximated by $\tilde{H}$, which is an RV following the Nakagami-m distribution with shape parameter

$$\tilde{m} = \frac{N\tilde{\Omega}I_0(\kappa)}{2I_0(\kappa) + 2I_2(\kappa) - 4\tilde{\Omega}I_0(\kappa)}, \tag{3}$$

and spread parameter

$$\tilde{\Omega} = \left(\frac{I_1(\kappa)\Gamma\left(m+\frac{1}{2}\right)\sqrt{\Omega}}{I_0(\kappa)\Gamma(m)\sqrt{m}}\right)^2, \tag{4}$$

where I_p is the modified Bessel function of the first kind and order p [13]. Therefore, the instantaneous received SNR γ_r of the proposed system can be expressed as

$$\gamma_r = \gamma_t C_0 G N^2 \left(\frac{d_0}{d_1d_2}\right)^2 \tilde{H}^2, \tag{5}$$

where γ_t is the transmit SNR. We consider an RV Z, which is equal to

$$Z = {d_1}^{-2}\tilde{H}^2, \tag{6}$$

where $\tilde{H}^2$ is a gamma distributed RV with shape parameter $k = \tilde{m}$ and scale parameter $\theta = \frac{\tilde{\Omega}}{\tilde{m}}$. Thus, the expression for γ_r can be rewritten as

$$\gamma_r = \gamma_t C_0 G N^2 Z \left(\frac{d_0}{d_2}\right)^2. \tag{7}$$

III. Performance Analysis

A. Outage probability of a uniformly-distributed sensor

Considering that the sensor is uniformly distributed inside a circular area with radius R and the UAV is hovering above the disk's center at height h, the distance d_1 between the sensor and the synergetic UAV-RIS system is also an RV. Thus, the cumulative density function (CDF) of d_1 can be calculated through [14] and expressed as

$$F_{d_1}(x) = \frac{x^2 - h^2}{R^2}, x \in \left[h, \sqrt{h^2+R^2}\right]. \tag{8}$$

Proposition 1: The outage probability of a uniformly-distributed sensor can be approximated as

$$\mathcal{P}_o \approx 1 - \frac{\theta}{R^2 w} \sum_{i=0}^{\hat{k}-1} \frac{\gamma\left(i+1, \frac{h^2+R^2}{\theta} w\right) - \gamma\left(i+1, \frac{h^2}{\theta} w\right)}{i!}, \tag{9}$$

where $i!$ is the factorial of i, $\gamma(\cdot)$ is the lower incomplete gamma function [13], $\hat{k} = \lfloor k \rfloor$, $w = \frac{\gamma_{\rm thr} d_2^2}{\gamma_t {d_0}^2 C_0 N^2}$ and $\gamma_{\rm thr}$ is the received SNR threshold value.

Proof: The outage probability can be derived through the CDF of Z which is given by

$$F_Z(x) = \int_{-\infty}^{\infty} F_{\tilde{H}^2}\left(\frac{x}{y}\right) f_{{d_1}^{-2}}(y)\, dy, \tag{10}$$

where $F_{\tilde{H}^2}$ is the CDF of $\tilde{H}^2$ and $f_{{d_1}^{-2}}$ is the PDF of RV ${d_1}^{-2}$, which equals to

$$f_{{d_1}^{-2}} = \frac{1}{(xR)^2}, x \in \left[\frac{1}{h^2+R^2}, \frac{1}{R^2}\right]. \tag{11}$$

Thus,

$$F_Z(x) = \int_{\frac{1}{h^2+R^2}}^{\frac{1}{h^2}} \frac{\gamma\left(k, \frac{x}{\theta y}\right)}{\Gamma(k)} \frac{1}{(yR)^2} dy, \tag{12}$$

where $\Gamma(\cdot)$ is the gamma function [13]. By approximating k with $\hat{k}$, the lower incomplete gamma function is rewritten as

$$\gamma\left(k, \frac{x}{\theta y}\right) \approx \left(\hat{k}-1\right)! \left(1 - e^{-\frac{x}{\theta y}} \sum_{i=0}^{\hat{k}-1} \frac{x^i}{(\theta y)^i\, i!}\right). \tag{13}$$

After some algebraic manipulations, the CDF of Z is derived. The outage probability is defined as

$$\mathcal{P}_o = \Pr(\gamma_r \le \gamma_{\rm thr}) = \Pr(Z \le w). \tag{14}$$

Considering (14), the outage probability can be calculated as in (9), which concludes the proof. ∎

B. HARQ protocol

In this section, we investigate the use of time diversity through the HARQ protocol and specifically HARQ$^{\rm IR}$ and HARQ$^{\rm CC}$, to enhance the performance of the proposed system. However, in order to reduce latency, we consider truncated HARQ$^{\rm IR}$ and truncated HARQ$^{\rm CC}$, limiting the number of retransmissions to a maximum of L.

In HARQ$^{\rm IR}$, the transmission starts with a fixed code rate and the data frame is transmitted with a small number of parity bits called incremental redundancy frame. If the data frame fails to be decoded correctly, the receiver asks for a retransmission by sending a non-acknowledgment message (NACK), otherwise it responds with an acknowledgment message (ACK). If decoding fails, the transmitter sends a new incremental redundancy frame, thus the coding rate is adapted to the channel fading conditions.

In HARQ$^{\rm CC}$, instead of using parity bits, the receiver stores the erroneous decoded frame and, then, sends a NACK. Once the message is retransmitted, the new message is combined with the stored one using maximum ratio combining (MRC) and the receiver tries to decode the combined message. This process is repeated for L rounds. It should be mentioned that, in the proposed communication system, it is assumed that no erroneous transmission of ACK and NACK messages exists.

Proposition 2: The outage probability of the proposed system, i.e., the outage probability of the L-th round, with HARQ^{IR} can be expressed as

$$\mathcal{P}_{oL}^{\rm IR} = \frac{\gamma\left(\hat{k}_{\rm IR}, \frac{1+\gamma_{\rm thr}}{\theta_{\rm IR}}\right)}{\Gamma\left(\hat{k}_{\rm IR}\right)}, \tag{15}$$

where $\hat{k}_{\rm IR} = \frac{A^{2L}}{(1+2A+B)^L - A^{2L}}$ and $\theta_{\rm IR} = \frac{(1+2A+B)^L - A^{2L}}{A^{2L}}$ and A, B are given, respectively, by

$$A = \gamma_t G C_0 N^2 \left(\frac{d_0}{d_2}\right)^2 \frac{\hat{k}\theta}{R^2} \left(\ln\left(h^2+R^2\right) - \ln\left(h^2\right)\right) \tag{16}$$

and

$$B = {\gamma_t}^2 G^2 {C_0}^2 N^2 \left(\frac{d_0}{d_2}\right)^4 \frac{\left(\hat{k}\theta^2 + \hat{k}^2\theta^2\right)}{R^2} \left[\frac{1}{h^2} - \frac{1}{h^2+R^2}\right]. \tag{17}$$

Proof: The outage probability of the L-th HARQ$^{\rm IR}$ round is defined as

$$\mathcal{P}_{oL}^{\rm IR} = \Pr\left(\sum_{i=1}^{L} \log_2\left(1 + \gamma_t G C_0 N^2 \left(\frac{d_0}{d_2}\right)^2 Z_i\right) \le R_t\right), \tag{18}$$

where $R_t = \log_2(1+\gamma_{\rm thr})$. (18) can be rewritten as

$$\mathcal{P}_{oL}^{\rm IR} = \Pr\left(\prod_{i=1}^{L} \left(1 + \gamma_t G C_0 N^2 \left(\frac{d_0}{d_2}\right)^2 Z_i\right) \le 1 + \gamma_{\rm thr}\right). \tag{19}$$

Utilizing the moment matching technique, $S_1 = \prod_{i=1}^{L}\left(1 + \gamma_t G C_0 N^2 \left(\frac{d_0}{d_2}\right)^2 Z_i\right)$ can be approximated by a gamma distributed RV with shape parameter $\hat{k}_{\rm IR} = {\mathbb{E}^2[S_1]}/{\rm Var}[S_1]$ and scale parameter $\theta_{\rm IR} = {\rm Var}[S_1]/\mathbb{E}[S_1]$. Therefore, we need to calculate the first and the second moment of S_1 which can be expressed as $\mathbb{E}[S_1] = \left[1 + \gamma_t G C_0 N^2 \left({d_0}/{d_2}\right)^2 \mathbb{E}[Z]\right]^L$ and $\mathbb{E}[{S_1}^2] = \Big[1 + 2\gamma_t G C_0 N^2 \left({d_0}/{d_2}\right)^2 \mathbb{E}[Z] + {\gamma_t}^2 G^2 {C_0}^2 N^2 \left({d_0}/{d_2}\right)^4 \mathbb{E}[Z^2]\Big]^L$. The moments of Z can be calculated as

$$\mathbb{E}[Z] = \int_{\frac{1}{h^2+R^2}}^{1/h^2} \hat{k}\theta x \frac{1}{(xR)^2} dx \tag{20}$$

and

$$\mathbb{E}[Z^2] = \int_{\frac{1}{h^2+R^2}}^{1/h^2} \left(\hat{k}\theta^2 x^2 + \hat{k}^2\theta^2 x^2\right) \frac{1}{(xR)^2} dx. \tag{21}$$

After some algebraic manipulations, the parameters $\hat{k}_{\rm IR}$ and $\theta_{\rm IR}$ are obtained and by utilizing the CDF of the gamma distribution, (15) is derived which concludes the proof. ∎

Proposition 3: The outage probability of the proposed system, i.e., the outage probability of the L-th round, with HARQ$^{\mathrm{CC}}$ is equal to

$$\mathcal{P}_{oL}^{\mathrm{CC}} = 1 - \frac{\theta}{R^2 w} \sum_{i=0}^{L\hat{k}-1} \frac{\gamma\left(i+1, \frac{h^2+R^2}{\theta} w\right) - \gamma\left(i+1, \frac{h^2}{\theta} w\right)}{i!}. \tag{22}$$

Proof: The probability of erroneous decoding in the L-th HARQ$^{\mathrm{CC}}$ round can be expressed as

$$\mathcal{P}_{oL}^{\mathrm{CC}} = \Pr\left(\gamma_t G l N^2 \sum_{i=1}^{L} \tilde{H}^2 \leq \gamma_{\mathrm{thr}}\right). \tag{23}$$

Utilizing the moment matching technique, $S_2 = \sum_{i=1}^{L} \tilde{H}^2$ can be approximated by a gamma distributed RV with shape parameter $\hat{k}_m = \mathbb{E}^2[S_2]/\mathrm{Var}[S_2]$ and scale parameter $\theta_m = \mathrm{Var}[S_2]/\mathbb{E}[S_2]$. After some algebraic manipulations, it can be found that $\hat{k}_m = L\hat{k}$ and $\theta_m = \theta$ and thus, we obtain (22) which concludes the proof. ∎

For every truncated HARQ protocol with L rounds, the average number of retransmissions $\bar{T}_r$ is given by [9]

$$\bar{T}_r = 1 + \mathcal{P}_o + .. + \mathcal{P}_o \mathcal{P}_{o2}^{V} ... \mathcal{P}_{o(L-1)}^{V} \tag{24}$$

where $V \in \{\mathrm{IR}, \mathrm{CC}\}$. It is obvious that the number of retransmissions can vary depending on the channel conditions. For example, in case where the channel fading conditions are good, one transmission could be sufficient for error-free decoding, whereas in the case of bad channel conditions, more retransmissions of the same message might be required to transmit it successfully. Therefore, the average system's throughput, when HARQ is utilized, can be expressed as

$$\bar{R}(x) = \frac{W \log_2(1+\gamma_{\mathrm{thr}})}{\bar{T}_r}\left(1 - \mathcal{P}_{oL}^{V}\right), \tag{25}$$

where W is the communication system's bandwidth. It should be mentioned that for the case of no HARQ, $\bar{T}_r = 1$ and $\mathcal{P}_{oL}^{V} = \mathcal{P}_o$.

IV. Numerical Results

A. Simulation setup

The analytical expressions presented in the previous sections are validated numerically in this section via Monte Carlo simulations with 10^5 realizations. We examine an uplink communication scenario where a UAV carrying an RIS is hovering at $h = 50$ m above a disk's center whose radius R is assumed to be equal to 20 m and the truncated HARQ$^{\mathrm{IR}}$ and HARQ$^{\mathrm{CC}}$ with $L = 3$ rounds are utilized, unless it is stated otherwise. Also, the reference distance d_0 is set at 1 m, the carrier's frequency $f_c = 865$ MHz, the system's bandwidth $W = 125$ kHz and the path loss exponent for both links is set as $n = 2$. Furthermore, it is assumed that the sensor-RIS link is affected from Nakagami-m fading where the shape parameter m is chosen to be equal to 3, due to the favorable characteristics of communication links between the sensor nodes and the UAV. However, due to the incapability of perfect CSI acquisition and the UAV fluctuations, the concentration parameter is selected as $\kappa = 1$. Moreover, we set the transmission SNR $\gamma_t = 93$ dB, whereas the SNR threshold value is set as $\gamma_{\mathrm{thr}} = 0$ dB. Finally, it is assumed that both sensor and AP are equipped with isotropic antennas, hence, $G = 1$.

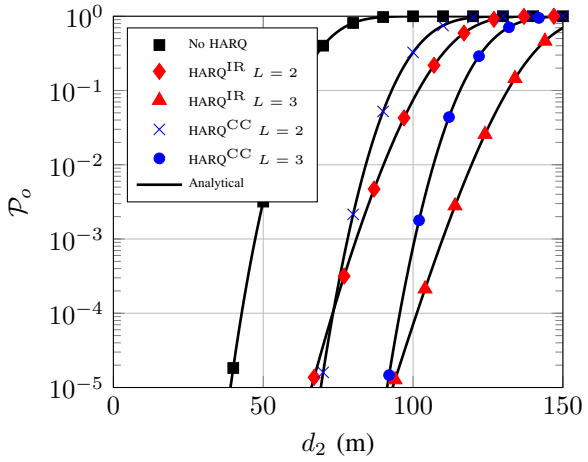

Fig. 2. Outage probability versus UAV-AP distance with $N = 150$.

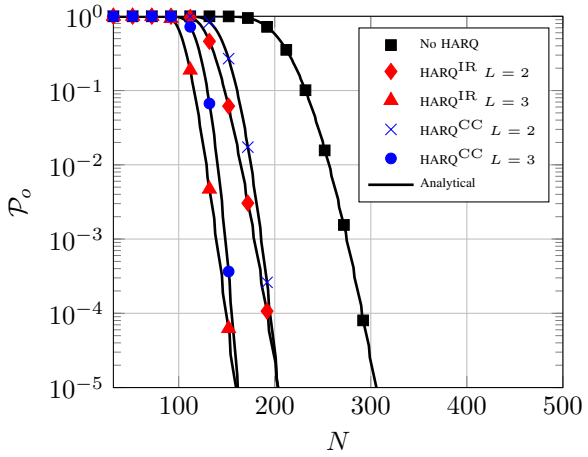

Fig. 3. Outage probability versus N for $d_2 = 100$ m.

B. Performance Evaluation

Fig. 2 illustrates the impact of the UAV-AP distance to the outage probability of the proposed synergetic UAV-RIS system for all the examined HARQ types and $N = 150$. As it can be observed, the utilization of both HARQ$^{\mathrm{IR}}$ and HARQ$^{\mathrm{CC}}$ can enhance the system's outage probability, which leads to a reliable transmission from the sensor to the AP, even in large UAV-AP distances. Moreover, it can be observed that leveraging the HARQ$^{\mathrm{IR}}$ protocol leads overall to increased UAV-AP distances with high-reliability compared to the HARQ$^{\mathrm{CC}}$ protocol, while having more retransmission rounds improves the successful reception for longer distances.

Following, in Fig. 3, we demonstrate the impact of the number of RIS's reflecting elements to the outage probability for $d_2 = 100$ m. As it can been seen, as the number of reflecting

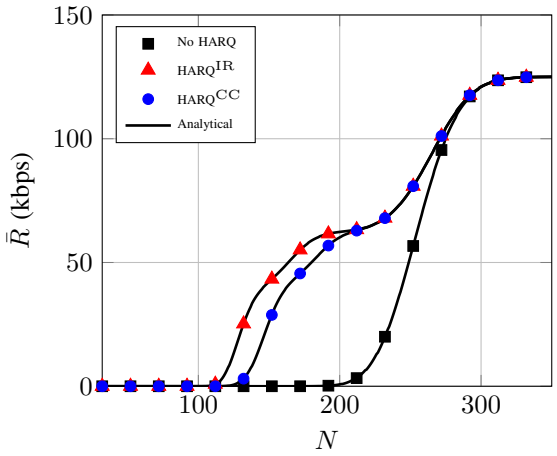

Fig. 4. Average throughput versus N for $d_2 = 100$ m.

elements increases, the outage probability is enhanced due to the fact that more reflecting elements take place into the signal's beamforming towards the AP. Furthermore, the outage probability can decrease even more by applying HARQ$^{\mathrm{IR}}$ or HARQ$^{\mathrm{CC}}$. As it is illustrated, HARQ$^{\mathrm{IR}}$ slightly outperforms HARQ$^{\mathrm{CC}}$ proving that the utilization of parity bits is a better option than the combination of the received message with the previous ones, which have been erroneously decoded.

Next, in Fig. 4, we demonstrate the system's average throughput versus the number of the RIS elements. Again, HARQ$^{\mathrm{IR}}$ outperforms HARQ$^{\mathrm{CC}}$ in terms of average throughput for $N \in [100, 200]$. In addition, we notice that the throughput saturates in all cases when $N \geq 300$, as it reaches the maximum achievable rate due to excellent channel conditions. Increasing N further than 300 would not only be unnecessary for the throughput, but it would also increase the UAV's power consumption due to the extra RIS weight, deteriorating the proposed system's energy efficiency. Finally, it should be mentioned that the shape of the HARQ curves in the $N \in [100, 250]$ range is caused by the fact that each consecutive retransmission leverages information from the previous one (i.e., due to the utilization of the parity bits and the MRC). In detail, as N decreases, the channel gain deteriorates and enables HARQ to initiate retransmission attempts to restore the communication. Thus, due to the different channel gain in every extra retransmission round, the average throughput behaves as in Fig. 4.

V. Conclusions

In this paper, we have investigated the communication performance of a data collection system consisting of randomly-deployed IoT sensors assisted by a UAV-mounted RIS. We have calculated the outage probability for two HARQ types, i.e., Incremental Redundancy and Code Combining, and provided useful metrics including the average number of retransmission and the average throughput. More specifically, we have demonstrated that, given a certain transmission rate, there is an upper limit in the performance for a specific number of elements, which is crucial due to the weight restrictions in UAV-assisted networks. Furthermore, it has been illustrated that, for low reflecting element density, HARQ$^{\mathrm{IR}}$ is able to provide slightly higher throughput compared to HARQ$^{\mathrm{CC}}$, whereas both HARQ protocols performed significantly better than the case where no HARQ was leveraged. Our future directions will combine the synergetic RIS-UAV system with a medium access control protocol to further improve the performance of an IoT network in an energy-efficient and cost-effective way.

Acknowledgements

This work has been funded by the European Union´s Horizon 2020 research and innovation programme under Grant Agreement No. 891515 (HERMES).

References

[1] F. Guo, F. R. Yu, H. Zhang, X. Li, H. Ji, and V. C. M. Leung, "Enabling Massive IoT Toward 6G: A Comprehensive Survey," *IEEE Internet Things J.*, vol. 8, no. 15, pp. 11 891–11 915, 2021.

[2] P. S. Bithas, V. Nikolaidis, A. G. Kanatas, and G. K. Karagiannidis, "UAV-to-Ground Communications: Channel Modeling and UAV Selection," *IEEE Trans. Wireless Commun.*, vol. 68, no. 8, pp. 5135–5144, Aug. 2020.

[3] D. Tyrovolas, S. A. Tegos, P. D. Diamantoulakis, and G. K. Karagiannidis, "Synergetic UAV-RIS Communication with Highly Directional Transmission," *IEEE Wireless Commun. Lett.*, pp. 1–1, 2021.

[4] P.-V. Mekikis and A. Antonopoulos, "Breaking the Boundaries of Aerial Networks with Charging Stations," in *ICC 2019*, 2019, pp. 1–6.

[5] S. A. Tegos, D. Tyrovolas, P. D. Diamantoulakis, C. K. Liaskos, and G. K. Karagiannidis, "On the Distribution of the Sum of Double-Nakagami-m Random Vectors and Application in Randomly Reconfigurable Surfaces," 2021. [Online]. Available: arxiv.org/abs/2102.05591

[6] C. Liaskos, S. Nie, A. Tsioliaridou, A. Pitsillides, S. Ioannidis, and I. Akyildiz, "A New Wireless Communication Paradigm through Software-Controlled Metasurfaces," *IEEE Commun. Mag.*, vol. 56, no. 9, pp. 162–169, 2018.

[7] S. Li, B. Duo, X. Yuan, Y.-C. Liang, and M. Di Renzo, "Reconfigurable Intelligent Surface Assisted UAV Communication: Joint Trajectory Design and Passive Beamforming," *IEEE Wireless Commun. Lett.*, vol. 9, no. 5, pp. 716–720, 2020.

[8] Q. Wu, J. Xu, Y. Zeng, D. W. K. Ng, N. Al-Dhahir, R. Schober, and A. L. Swindlehurst, "A Comprehensive Overview on 5G-and-Beyond Networks with UAVs: From Communications to Sensing and Intelligence," 2021. [Online]. Available: arxiv.org/abs/2010.09317

[9] A. Chelli, E. Zedini, M.-S. Alouini, M. Pätzold, and I. Balasingham, "Throughput and Delay Analysis of HARQ With Code Combining Over Double Rayleigh Fading Channels," *IEEE Trans. Veh. Technol.*, vol. 67, no. 5, pp. 4233–4247, 2018.

[10] Q. Cao, H. Zhang, Z. Shi, H. Wang, Y. Fu, G. Yang, and S. Ma, "Outage Performance Analysis of HARQ-Aided Multi-RIS Systems," in *2021 IEEE WCNC*, 2021, pp. 1–6.

[11] Q. Wu and R. Zhang, "Intelligent Reflecting Surface Enhanced Wireless Network via Joint Active and Passive Beamforming," *IEEE Trans. Wireless Commun*, vol. 18, no. 11, pp. 5394–5409, Nov. 2019.

[12] M.-A. Badiu and J. P. Coon, "Communication Through a Large Reflecting Surface With Phase Errors," *IEEE Wireless Commun. Lett.*, vol. 9, no. 2, pp. 184–188, 2020.

[13] I. S. Gradshteyn and I. M. Ryzhik, "Table of integrals, series, and products." *Academic press*, 2014.

[14] V. K. Papanikolaou, G. K. Karagiannidis, N. A. Mitsiou, and P. D. Diamantoulakis, "Closed-Form Analysis for NOMA With Randomly Deployed Users in Generalized Fading," *IEEE Wireless Commun. Lett.*, vol. 9, no. 8, pp. 1253–1257, 2020.